Fire behaviour of liquid solvents for energy storage applications

Process Safety and Environmental Protection 188 (2024) 726–734

Contents lists available at ScienceDirect

Process Safety and Environmental Protection

journal homepage: www.journals.elsevier.com/process-safety-and-environmental-protection

Fire behaviour of liquid solvents for energy storage applications

Benedetta Anna De Liso, Gianmaria Pio *, Ernesto Salzano

Department of Civil, Chemical, Environmental and Materials Engineering, Alma Mater Studiorum - University of Bologna, Bologna 40131, Italy

ARTICLE INFO

Keywords:
Pool fire
Liquid solvent
Flaming
Smouldering
Rate of heat generation
Supercapacitor
Battery

ABSTRACT

The introduction of innovative solutions for the energy supply chain is promoting the use of batteries and supercapacitors, posing new challenges from a safety point of view. This work presents bench-scale experiments devoted to the evaluation of the fire behaviour of liquid solvents, employing an in-house procedure for the characterization of the ignition and flame behaviour of liquids either in the presence or absence of ignition sources. Different boundary conditions were tested to identify the most suitable set of values for a standardized assessment of safety parameters for acetonitrile, ethyl acetate, lactic acid, and hexane. The produced vapours and the exhaust gas were analysed together with the evolution in time of the rate of heat generation. The fire behaviour was quantified in terms of time to reach the maximum value of the heat release rate and the peak. The former is related to the flash point, whereas the latter is determined by the thermodynamics and kinetics of the investigated species. In addition, the overall rate and the ruling regimes (e.g., smouldering or flaming) were determined based on the collected data. The comparison between the obtained values and the typical velocities attributed to vaporization, mixing, and gas-phase reactions suggests that vaporization can be considered as the rate-determining step only in the case of flaming.

1. Introduction

The need for a sustainable supply chain for energy production has promoted the electrification of several industrial sectors, imposing the development of alternative solutions in terms of energy storage systems, as well. Indeed, a large share of the successful implementation of electric vehicles is related to the development of suitable energy storage systems (Lin et al., 2021). In addition, a possible penetration of supercapacitors and fuel cells has been forecasted by Winter and Brodd (2004) for markets currently occupied by traditional batteries, as well. In this sense, it is worth mentioning that electrical storage technologies can be mostly differentiated based on the model, composing material, or adopted solvent (Tan et al., 2017). The last parameter has been recently indicated as an essential aspect to be considered toward the optimization of the alternative solutions (Bu et al., 2023), thus it has been considered the subject of intensive research for the identification of a sustainable solvent for its implementation in fast-charging batteries (Ben Talouba et al., 2018). Small esters including methyl acetate, ethyl acetate, and methyl propionate have been typically analysed as possible solvents or co-solvents (Logan et al., 2018). Alternatively, acetonitrile solutions have been indicated as promising solutions because of the elevated chemical and oxidative stability together with the elevated conductivity (Yamada et al., 2014; Zhang et al., 2021). More recently, hexane has been introduced as a possible alternative to chemically and physically improve the energy density of batteries (Cheng et al., 2023) as well as the use of quasi-solid-state gel based on lactic acid (Chai et al., 2022). Regardless of the mentioned species, most of the studies performed so far have been focused on the characterization and optimization of the technical performances as well as production processes, with poor or limited knowledge of the safety parameters of the involved species and mixtures. Nevertheless, the presence of liquid organic solvents can result in additional accidental scenarios to be considered, e.g., fires and release of toxic vapour. In this framework, a complete understanding of the physical-chemical behaviour ruling the ignitability and flame properties of liquids based on dedicated experimental campaigns is paramount to assess safety and overall sustainability aspects of any solution (Fernandes Oliveira et al., 2019).

The experimental characterization of the most relevant safety parameters can be performed utilizing different systems as well as by investigating different scales (Cao et al., 2020). Among the parameters of interest, it is worth mentioning the time to ignition (t_i), the heat release rate profile (HRR) and peak (pHRR), the corresponding time (tpHRR), the mass loss rate profile (MLR) and mean (mMLR). A well-established system for the experimental campaigns at bench scale is

* Corresponding author.
E-mail address: gianmaria.pio@unibo.it (G. Pio).

https://doi.org/10.1016/j.psep.2024.05.153
Received 24 November 2023; Received in revised form 24 May 2024; Accepted 31 May 2024
Available online 2 June 2024

the cone calorimeter, being widely adopted for the assessment of fire and flammability behaviour of materials (Bray et al., 2023). Although the basic principles and standard procedures are detailed and described in the dedicated literature (British Standards Institution, 2019), a brief overview is provided below for completeness. The cone calorimeter operates on the principle of exposing a sample to a controlled external radiant heat source generated by a cone-shaped heater, within the range of 0–100 kW/m^2. The mass of the sample, the heat release rate, the flow rate and oxygen concentrations in the exhaust gas are monitored in time (Babrauskas, 1984; Brohez et al., 2000). Based on the collected data, the amount of oxygen consumed by the reaction is calculated. Hence, the principle of heat release is adopted to obtain the net heat of combustion. Besides, the cone calorimeter provides additional valuable data, such as the total heat release (THR), the mass loss rate (MLR), the smoke production (SPR), and other fire-related parameters. Smoke obscuration is measured as the fraction of laser light intensity that is transmitted through the smoke in the exhaust duct. This fraction is used to calculate the extinction coefficient according to Bouguer's law (Babrauskas, 1989). The assessment of the time to autoignition (TTa) is also possible, being the interval from starting the process of exposure and the point at which sustained flaming can be observed (neglecting flames on the surface of the specimen lasting less than 5 s). This parameter is largely influenced by the external heat flow and the thermal properties of the analysed specimen, particularly thermal inertia, which derives from the traditional theory of solid heat conduction (Janssens, 1991; An et al., 2015). In general, an external heat flux value lower than 20 kW/m^2 is used to investigate ignition and flammability, while a range of 25 – 30 kW/m^2 may be used to investigate fire spread. Furthermore, external heat flux larger than 50 kW/m^2 can be used to examine compartment fires following flashover and to test combustion parameters (Mun et al., 2021).

The ignitability of liquid fuels has traditionally been evaluated based on the properties of their vapours, namely autoignition temperature (AIT) and minimum ignition energy (MIE). Both parameters can be tested employing standard apparatus and specified test conditions (Beyler, 2003). However, these characteristics do not apply to the piloted ignition of a fixed-volume, calm, and confined liquid pool. Therefore, the influences of the implemented protocol should be carefully considered once the obtained results are applied to the evaluation of pool fire scenarios. Besides, they cannot be used for a simultaneous evaluation of the produced thermal power. In this view, the definition of alternative standardized protocols representative of fire conditions of liquids, suitable for the characterization of their flammability and safety parameters, is paramount, as indicated in the current literature (Chakrabarty et al., 2016). According to the cited standards (British Standards Institution, 2019; ASTM, 2023), the cone calorimeter can be used to characterize the fire performance of solids according to their propensities for ignition, boiling, and burning, as well as their combustion characteristics. Considering the nature of the hypothesis and procedures typically adopted, these principles can be extended also to the characterization of species at a liquid phase. Nevertheless, a limited amount of data on liquids can be found in the literature, with often inconsistent procedures (DiDomizio et al., 2021).

Once considering the numerical approach, the effects of boundary conditions on the overall reactivity can be assessed through dedicated kinetic mechanisms (Pio and Salzano, 2018). The overall reactivity of liquid substances can be expressed in terms of laminar burning velocity or mass burning rate (Gu et al., 2000). In the former case, the required production and collection of a vaporized stream can be obtained by dedicated heating and pumping systems acting on bulk as well as on droplets, as discussed in detail in the recent literature (Broustail et al., 2011; McGrath et al., 2023; Yin et al., 2023). A flowing (or evaporating) condition is required to determine the laminar burning velocity (Marshall et al., 2011). Conversely, the determination of the mass burning rate is commonly realized under quiescent conditions, reproducing a completely formed liquid pool (Sung et al., 2021).

The realization of a robust database collecting safety parameters for liquid solvents can be intended as a crucial step toward the evaluation of inherent safety aspects and sustainability of industrial processes as well as the identification of the optimized design and conditions, as recently suggested in the current literature for species under consideration in this work (Janošovský et al., 2022; Zhai et al., 2023). In addition, understanding the kinetic aspects ruling the chemical phenomena of solvents suitable for energy storage systems at different external heat fluxes provides essential information for the evaluation of typical scenarios involving batteries, including runaway reactions (Tang et al., 2023) with obvious implications in the field of process safety and risk engineering. Under these premises, this work presents an experimental campaign, based on the use of a cone calorimeter, devoted to the realization of a robust and comprehensive dataset on the ignition and burning propensity of possible components of innovative energy storage systems. Indeed, the realization of an accurate and robust procedure for the characterization of liquid systems is essential to provide further insights on the subject and allow the identification of the most suitable solutions. Obtained measurements were compared with numerical estimations accounting for the chemical kinetics to identify the rate-determining step of heterogeneous reactions.

2. Experimental set-up and procedure

The current work presents an experimental campaign conducted on a bench scale for the characterization of liquid organic species utilizing a cone calorimeter. The tests were conducted based on the experimental setup described in ISO 5660 or ASTM E1354 (Marsh and Gann, 2013). The main steps and the adaptations required for the analysis of liquid species are reported in this section. A schematic representation of the adopted cone calorimeter is reported in Fig. 1. The main components are I) a sample holder with a conical form made of non-combustible metallic material; II) a conical-shaped resistance providing a given heat flux; III) an electric ignition source located at the top of the heating cone resistance; IV) heat flux sensors located around the sample holder to detect the heat release rate (HRR) produced by the burning substance; V) an air supply system providing a constant flow rate of 24 l/s; VI) an evacuation system venting the exhaust gases; VII) a load cell measuring the mass loss rate of the sample during the test; VIII) a photometer laser beam detecting the rate of smoke production and the fraction of particulate matter produced during the combustion processes.

In this work, the tests were conducted by using a layer of insulating material and aluminium foil in the sample holder. The tested materials were: acetonitrile ($\geq$ 99.5 %v), lactic acid ($\geq$ 90 %v), ethyl acetate ($\geq$ 99.5 %v) and hexane ($\geq$ 99 %v). An initial sample surface of 0.01 m^2, an initial sample thickness of 0.01 m, a distance between the sample and the heating element of 0.025 m, and a horizontal orientation of the cone heater were kept constant for the whole set of experiments. Conversely, different tests were performed at constant heat flux within the range of 7 – 50 kW/m^2.

In the case of the absence of immediate ignition, a sparkling ignition was provided with a time interval of 50 s to evaluate the ignitability of the investigated solvents. The precision and reproducibility of the measurements were ensured by following the prescribed procedures and using the proper equipment. The experimental setup described in this section provides a framework for further data analysis and interpretation, allowing for the study objectives to be addressed and valid conclusions to be drawn.

The results of this work were discussed and analysed using the physical and thermodynamic properties listed in Table 1, with 298 K and 1 atm as reference temperatures and pressures, (Cameo, 2023; Linstrom and Mallard, 2014; Perry et al., 2007).

Besides, the measured compositions of the exhaust gas were employed for the evaluation of the combustion efficiency (CE), following the definition provided in the literature (Ward and Hardy, 1991) and reported in Eq. (1) for the sake of clarity.

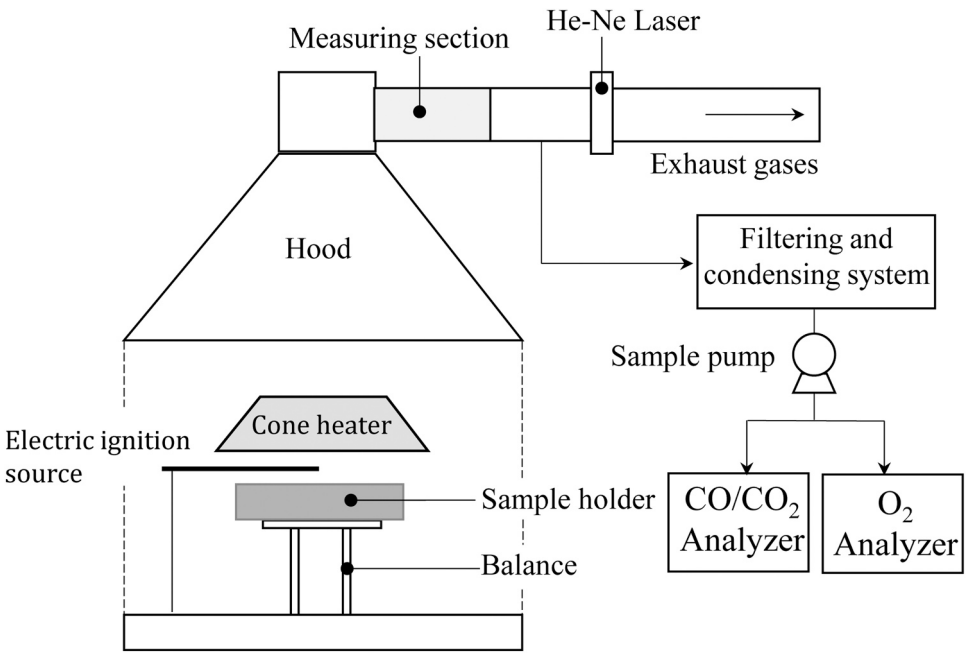

Fig. 1. Schematic representation of the experimental system adopted in this work.

Table 1
Thermochemical properties of acetonitrile, ethyl acetate, lactic acid and hexane, at 298 K and 1 atm, unless otherwise noted. Autoignition temperature (T_a), flash point temperature (T_F), bubble point temperature (T_B), thermal conductivity (k_L) and density of the liquid solvent (ρ_L) respectively (Cameo, 2023; Linstrom and Mallard, 2014; Perry et al., 2007).

Component	T_a [°C]	T_F [°C]	T_B [°C]	k_L [W/mK]	ρ_L [kg/m^3]
Acetonitrile	523.9	5.5	81.6	0.120	777
Ethyl Acetate	426.7	-4.0	77.2	0.193	894
Lactic Acid	> 400	110.0	216.0	0.144	1200
Hexane	224	-23.0	68.9	0.203	656

$$CE = \frac{[C]_{CO_2}}{[C]_{CO} + [C]_{CO_2} + [C]_{HC} + [C]_{PC}} \quad (1)$$

where [C] represents the amount of carbon C in mass emitted by the species reported as subscript (HC stands for unburned hydrocarbons and PC for particulate). This definition of combustion efficiency allows for the identification of the conditions leading to the transition from a smouldering phase to a flaming phase. Indeed, CE = 90 % is typically considered as the threshold value for this transition (Ferek et al., 1998). This aspect is particularly significant for safety applications because smouldering might not be as easily detected as flaming fires, making the combustion process persist for an extended period without drawing attention potentially resulting in hidden fire or lingering source of ignition. Following this hypothesis, a critical external flux leading to the transition from smouldering to flaming regimes (q_{StF}) was defined based on the CE resulting from data collected in this work at the time corresponding to the peak in heat release rate.

Based on the collected peak in the mass loss rate (pMLR), the density of the fluid (ρ), and the sample surface (A), the peak in the overall reaction rate (pORR) was defined as in Eq. (2). Data were calculated for the investigated species as a function of the adopted boundary conditions.

$$pORR = \frac{pMLR}{A \bullet \rho} \quad (2)$$

3. Results and discussion

Fig. 2 presents the time evolution of the heat release rate (HRR) collected in this work for the investigated solvents exposed to different external fluxes (included within the range of 7 – 50 kW/m^2). It is worth considering that fluxes larger than 25 kW/m^2 result in almost immediate and complete combustion in the case of hexane, making the collection of robust data unfeasible once exposed to larger radiative fluxes. Conversely, the lactic acid does not produce a stable flame once exposed to fluxes equal to or smaller than 15 kW/m^2, thus this value can be intended as the critical heat flux leading to the ignition of lactic acid, according to the definition reported in the literature (Rantuch et al., 2021).

The comparison of the collected HRR profiles along with the time indicates that either the intensity or the duration of the peaks are significantly affected by the provided flux regardless of the analysed compound. Nevertheless, hexane shows a shorter delay time and a more intense peak in heat release than the other compounds analysed in this work, regardless of the provided heat flux. Once the remaining compounds are analysed, different trends can be distinguished if the peak in heat release rate and the corresponding time are compared. More specifically, ethyl acetate shows a smaller ignition time than acetonitrile although a less intense peak is detected once heat fluxes larger than 7 kW/m^2 are provided to the sample. The observed trend for the time corresponding to the peak in the heat release rate can be related to the different flash points and autoignition temperatures of the investigated species, resulting in the formation of flammable vapours in less severe conditions during the tests for any given time. More specifically, according to Cameo (Cameo, 2023), the flash point and the autoignition temperatures of the investigated species are respectively: 5.5 °C and 523.9 °C for acetonitrile, −4 °C and 426.7 °C ethyl acetate, 110 °C and >400 °C lactic acid, and −23 °C and 224 °C hexane.

The observed trend in peak heat release rate can be intended as a result of the combination of thermodynamic and kinetic aspects involving the investigated species. The former can be directly associated with the heat of combustion per unit of mass, being −30.63 kJ/g, -25.64 kJ/g, −14.93 kJ/g, and −48.41 kJ/g respectively for acetonitrile, ethyl acetate, lactic acid, and hexane (Linstrom and Mallard, 2014). The latter can be quantified in terms of the peak in the mass loss rate (pMLR),

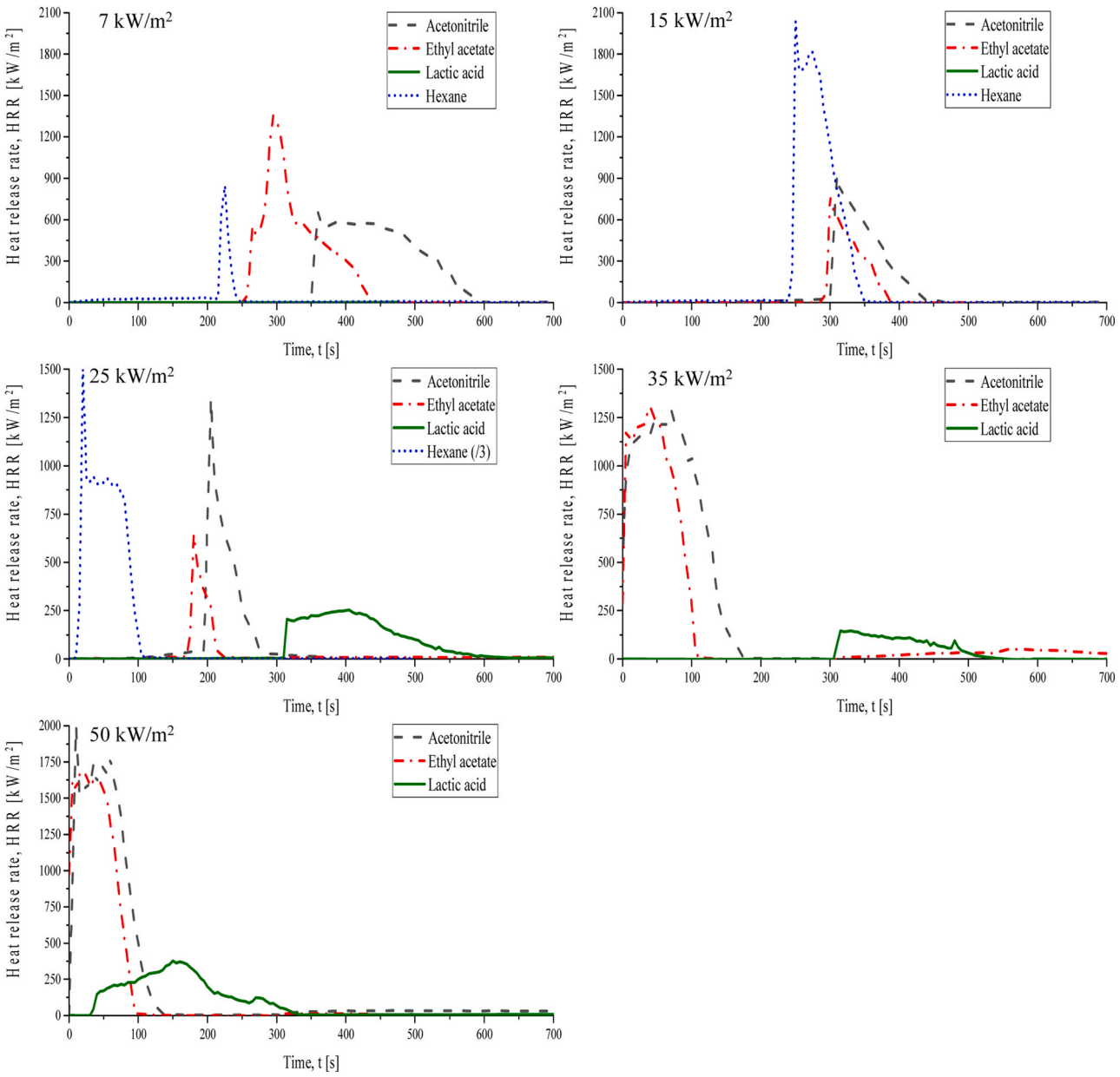

Fig. 2. Heat release rate profiles measured by cone calorimeter tests of acetonitrile, ethyl acetate, lactic acid, and hexane exposed to an external flux of 7, 15, 25, 35, and 50 kW/m^2. Please note that data collected during the hexane test were divided by a factor of 3 for the heat flux of 25 kW/m^2 for the sake of visualization.

whose profiles are reported in Fig. 3 and Fig. 4 for the tests conducted at 15 kW/m^2 and 25 kW/m^2, respectively.

The mass loss rate (MLR) curves of the analyzed solvents exhibit different phases. In the pre-ignition phase, before combustion starts, the MLR is relatively low as the liquid absorbs heat and begins to vaporize. Once the liquid reaches its ignition temperature the MLR starts to increase as the combustion process becomes established and the liquid releases more volatile components. In the steady burning, the MLR stabilizes at a relatively constant rate, indicating a sustained and stable combustion process. After the peak, the rate may decrease slightly due to the depletion of volatile components or changes in the combustion process. As the combustion process nears completion, the MLR approaches zero, indicating that all the available fuel in the liquid has been consumed. Hexane unlike other solvents investigated in this work is characterized by a sudden growth of MLR and an equally rapid flame out leading to a non-negligible solvent residue. As reported in the literature (DiDomizio et al., 2021) the mass loss rate of a liquid sample is typically influenced by the thickness (σ). In instances of a limited fuel quantity, the liquid swiftly attains the boiling temperature after ignition. Conversely, when the fuel quantity is substantial, a state of thermal equilibrium can be achieved, leading to a relatively consistent burning rate. As heat permeates through the liquid affecting the temperature profile within the liquid bulk and a large section of the volume reaches the boiling temperature, a rapid transition to boiling combustion may occur. This phenomenon is propelled by the reliance of heat flux on the overall heat transfer coefficient. However, an additional consideration that must be taken into account is the influence of the thermal conductivity (k_L) of the specific fuel on the heat transfer coefficient. By deriving the thickness of the sample from the measured mass and assuming the thermal conductivity of the solvents at a reference temperature (Crowl et al., 2008) σ / k_L profiles of the solvent over time were obtained. Hexane is characterized by a sudden boiling combustion and a relevant decrease of σ / k_L ratio, with respect to the other investigated solvents. These discrepancies can be evaluated in the light of additional elements such as the time of the peak in the heat release rate (tpHRR) and the peak in the heat release rate (pHRR), the ratio between CO and

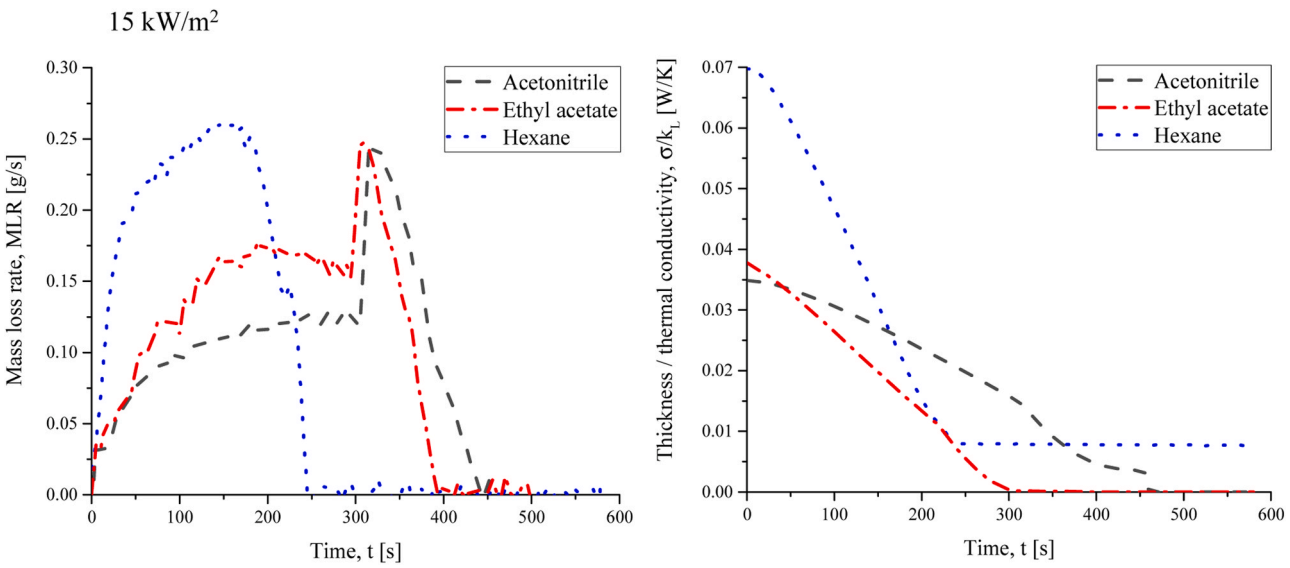

Fig. 3. Mass loss rate profiles (left) and thickness / thermal conductivity ratio (right) over time for each solvent at 15 kW/m^2.

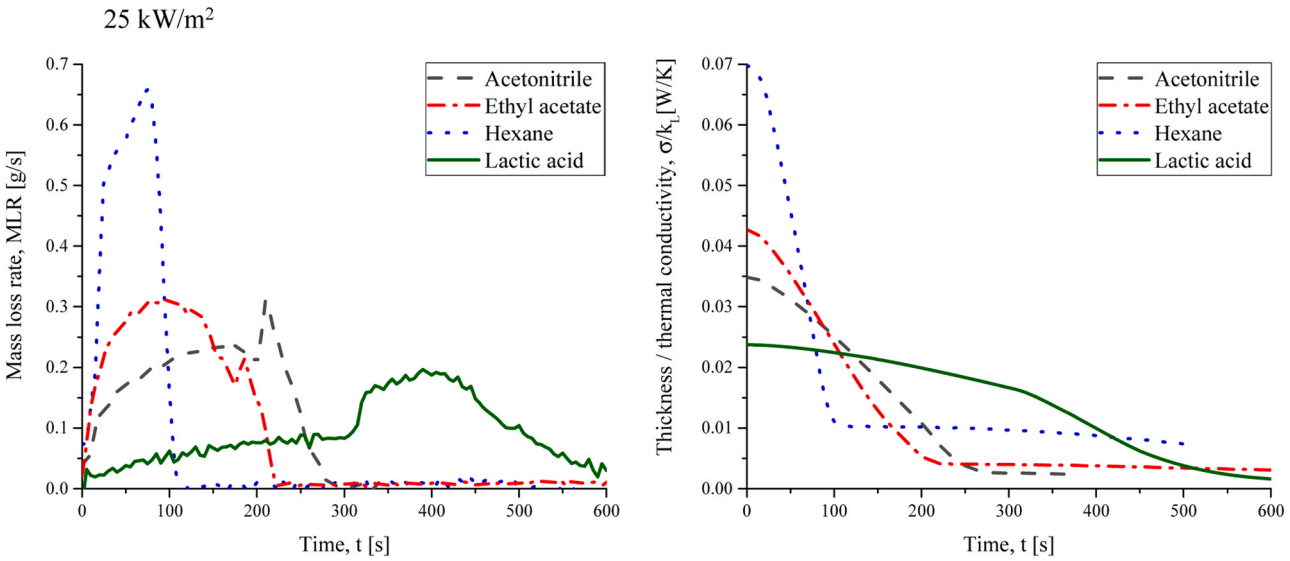

Fig. 4. Mass loss rate profiles (left) and thickness / thermal conductivity ratio (right) over time for each solvent at 25 kW/m^2.

CO_2 yields, and pMLR reported in Table 2.

Although lactic acid shows lower reactivity, as demonstrated by the large values of tpHRR, the smallest COY/CO_2Y ratio is reported for this compound. This ratio can be considered as directly connected to the CE previously defined in Eq. (1). Based on the gathered measurements, a q_{StF} can be obtained for acetonitrile and ethyl acetate, only, being equal to 7 kW/m^2 and 25 kW/m^2, respectively. Remarkably, the lowest pHRR for ethyl acetate is reported at the q_{StF}, although smaller external fluxes were tested. For the remaining species (i.e., hexane and lactic acid) a proper smouldering regime cannot be observed, as confirmed by CE significantly larger than 90 % for all the investigated conditions. This trend can be intended as a combination of the main phenomena characterizing liquid-gas reactive systems: evaporation, mixing, and gas-phase reaction. More specifically, since smouldering is favoured by a limited supply of oxygen with respect to the flammable vapours, disproportions between evaporation rates and gas phase kinetics can determine the overall smouldering combustion process. Indeed, an intrinsic tendency to undergo complete combustion can be assumed for lactic acid due to the chemical structure characterized by an elevated ratio between O/C, regardless of the evaporation rates. This hypothesis is supported by the values collected for the acetonitrile, which is more prone to incomplete combustion leading to CO production, having a structure characterized by a triple bond C-N and the absence of oxygen, but at the same time more volatile based on the normal boiling point than lactic acid. In this light, it is also worth noting that hexane and ethyl acetate show similar COY/CO_2Y values but different flaming behaviour. Besides, only the latter species has an oxygenated group within the chemical structure. This discrepancy can be associated with the large reactivity of hexane, demonstrated by a tpHRR smaller by almost an order of magnitude than the other species investigated in this work, promoting the direct conversion of CO to CO_2 (Wang et al., 2020). In this view, the peak in the overall reaction rate (pORR) is reported in Table 3 as a function of external heat flux and investigated components.

Considering the typical aspects involving a heterogeneous reaction, the kinetics of the combustion mechanism of a liquid solvent can be affected by different phenomena occurring during the process. The liquid vaporization, the mixing of vapour with the surrounding air forming a flammable cloud, and the gas-phase reactions were analysed.

Table 2
Summary of the main parameters experimentally collected in this work in the case of external flux of 25 kW/m^2.

Component	Heat flux [kW/m^2]	pHRR [kW/m^2]	tpHRR [s]	COY/ CO_2Y [-]	pMLR [g/s]
Acetonitrile	7	658.25	360	0.014	0.202
	15	925.93	310	0.039	0.246
	25	1348.00	205	0.087	0.310
	35	1290.26	70	0.072	0.441
	50	1998.30	10		
Ethyl acetate	7	1352.42	295	0.007	0.562
	15	767.23	300	0.012	0.248
	25	645.00	180	0.032	0.320
	35	1308.04	40	0.008	0.527
	50	1672.52	25		
Lactic acid	7	2.07	475	0.004	0.030
	25	255.00	405	0.016	0.120
	35	146.24	330	0.037	0.200
	50	375.28	150	0.275	0.020
Hexane	7	2039.76	250	0.075	0.366
	15	847.31	225	0.040	0.260
	25	255.00	405	0.016	0.120

pHRR = Peak of heat release rate; tpHRR = Time of the peak of heat release rate; CO/CO_2 = ratio of CO and CO_2 yields; pMLR = Peak of mass loss rate.

Table 3
Peak of overall reaction rate of acetonitrile, ethyl acetate, lactic acid and hexane at different heat flux conditions.

Component	Heat flux [kW/m^2]	pORR ($\bullet 10^{-5}$) [m/s]
Acetonitrile	7	0.98
	15	1.41
	25	1.82
	35	3.89
	50	4.68
Ethyl Acetate	7	1.56
	15	1.76
	25	1.14
	35	3.38
	50	3.20
Lactic Acid	7	0.06
	25	0.58
	35	0.98
	50	1.39
Hexane	7	1.33
	15	1.29
	25	4.36

A schematic representation of these phenomena is provided in Fig. 5.

In this sense, it is convenient to define different velocities representative of the listed phenomena to identify the rate-determining step. As mentioned before, based on the exchanged heat flux, different regimes can be observed for the liquid-to-vapour transition, determining the overall heat transfer coefficient (Incropera et al., 2007). Hence, the model as well as the value of the rate of vaporization can be affected by the provided heat flux. Conversely, the mixing rate can be mostly related to the turbulence of the surrounding atmosphere (Gavelli et al., 2008). Once the gas phase is of concern, the overall reactivity is typically quantified utilizing the laminar burning velocity in the case of low initial temperatures (Salzano et al., 2018) if a flaming regime is reached. Alternatively, specific analyses of the smouldering rate are necessary (Hagen and Meyer, 2021). To determine the influences of each mentioned step, data obtained under different heat flux conditions were compared. For all the investigated conditions values smaller than 10^{-5} m/s were observed. Hence, it is possible to conclude that the gas-phase chemistry assumes a negligible impact on the overall reaction rate being the typical laminar burning velocity of the investigated species $\sim 10^{-2}$ m/s, as reported in the experimental analyses retrieved in the current literature for the case of hexane and ethyl acetate (Coronel et al., 2013; Kumar et al., 2023). Generally speaking, it was possible to observe that the overall reaction rate slightly increased with the heat flux. More specifically, a linear behaviour was observed for acetonitrile and lactic acid. This is particularly relevant since the peak values are considered for the calculation of the overall reaction rate. Indeed, this allows for the achievement of the nucleate boiling regimes under the investigated conditions, meaning that the same model can be considered for the estimation of the overall heat transfer coefficient (Vesovic, 2007). Hence, based on the observed trend, the vaporization can be assumed as the rate-determining step under the investigated conditions. Conversely, the minimum pORR was observed at 25 kW/m^2 for the ethyl acetate. This value corresponds to the previously identified critical flux resulting in the transition from smouldering to flaming regime. Bearing in mind that smouldering can be associated with a deficiency, even locally, in oxygen content, evaporation cannot be considered a rate-determining step in the case of low heat flux. Indeed, poor mixing is more likely to cause the conditions leading to smouldering with a consequence reduction in pORR because of the less effective combustion at low temperatures. Once the external heat flux is increased, a nucleate boiling regime can be assumed, in agreement with previous considerations on the investigated liquids, resulting in an enhanced mixing due to the presence of bubbles. The abovementioned conditions result in the smouldering to flaming transition, which has positive feedback on the generated power (namely higher combustion efficiency) and overall reaction rates.

To assess the ignitability and the reactivity of each solvent, a source of ignition (electric sparkle) was provided with a time interval of 50 s and three different traffic light charts are reported in Table 4, Table 5

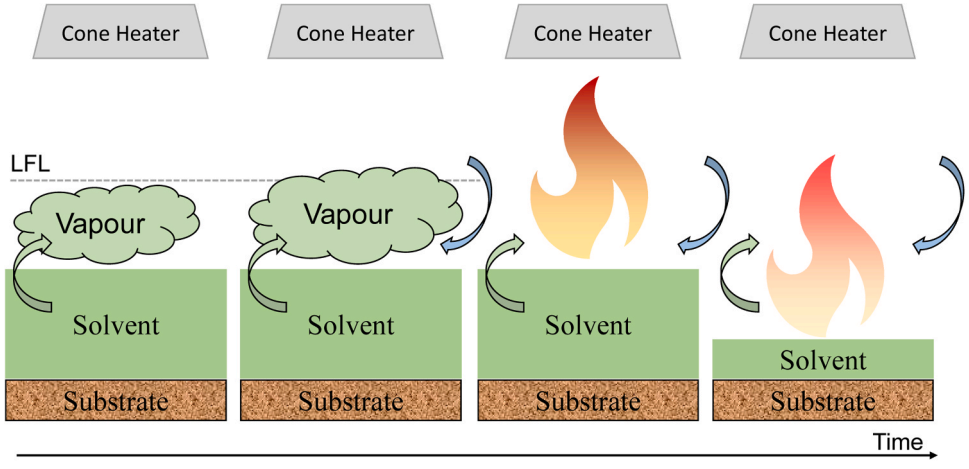

Fig. 5. Schematic representation of the main phenomena characterizing the reactive systems investigated in this work.

Table 4
Ignitability of the tested samples after ignition within the time interval [50 s; 250 s[observed experimentally in this work.

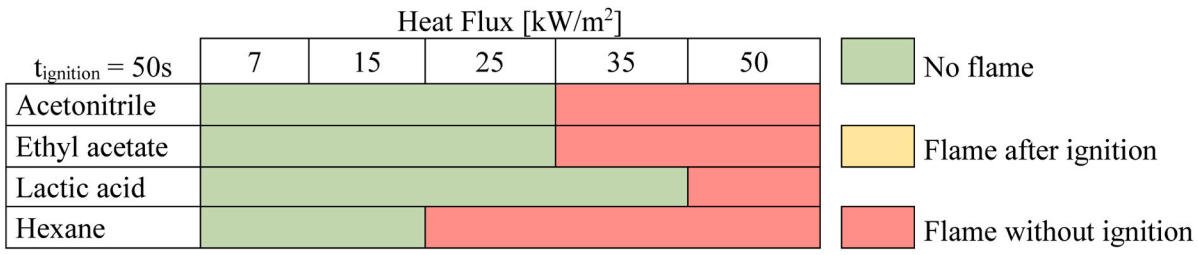

Table 5
Ignitability of the liquid samples after ignition within the time interval [250 s; 350 s[observed experimentally in this work.

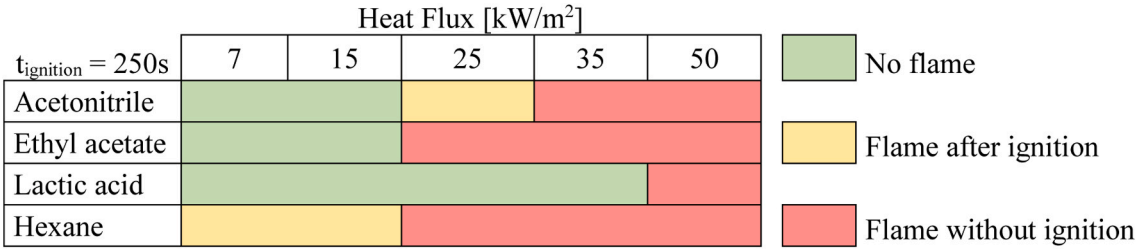

Table 6
Ignitability of the liquid samples after ignition at 350 s observed experimentally in this work.

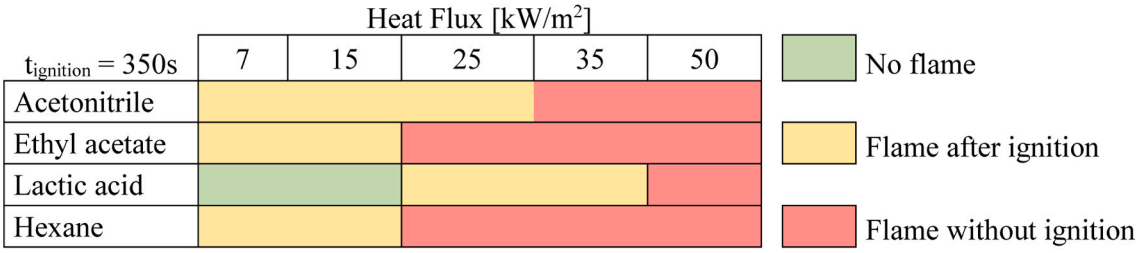

and Table 6, by considering different intervals of ignition.

The experimental data clearly show that acetonitrile exhibits distinct ignition patterns depending on the heat flux. At 7–15–25 kW/m^2 it only ignites when subjected to external ignition sources, taking approximately 350 s to catch fire. However, at higher heat fluxes (35–50 kW/m^2), acetonitrile ignited spontaneously without any external ignition stimulus. Similar behaviours are also evident in ethyl acetate, which demonstrates ignition properties akin to acetonitrile under both low and high heat flux conditions. Conversely, lactic acid has proven to be the singular non-flammable solvent at low thermal fluxes, even enduring an ignition after 350 s. In stark contrast, hexane ranks as the most flammable solvent within the studied set. The data unequivocally demonstrate that it is capable of autoignition after a mere 50 s at heat fluxes of 25–35–50 kW/m^2.

The comparison of the reported data revealed a clear correlation between the ignition time and the ignitability of the liquid fuel. The longer the ignition time recorded for a particular fuel, the higher its ignitability. This suggests that fuels with longer ignition times have a greater susceptibility to catch fire easily and sustain combustion due probably to the required mixing time which mainly influences the combustion mechanism. By examining the reactivity of different solvents, the data indicated that lactic acid exhibited a lower level of reactivity compared to the other solvents tested. These findings suggest that lactic acid is less prone to undergoing chemical reactions in the given experimental conditions. Its molecular structure or specific chemical properties may contribute to its lower reactivity. In contrast, hexane displayed the highest reactivity, becoming the most flammable and unsafe solvent among the other fuels.

4. Conclusions

The aim of the presented experimental campaign was to assess the response of the liquid samples to varying heat fluxes, which represent the possible thermal exposure from an external fire source. Overall, the experimental tests conducted provided valuable data on the influence of external heat fluxes on the ignition characteristics of liquid samples. The key parameters for the characterization of the fire behaviour of liquid solvents were compared against the main properties of the investigated species, showing that the ignition delay time can be directly related to the flash point, whereas the maximum heat release rate is a combination of thermodynamic and kinetic parameters. The overall reactivity was determined based on the collected data together with the production of the main species in the exhaust gas. The gathered information can be also used for the implementation of kinetic mechanisms in advanced

numerical models, including computational fluid dynamics. The conditions leading to the transition from smouldering to flaming regimes were identified, restricting the possible causes and conditions leading to the generation of second cascading events derived from undetected flames. Therefore, the collected data can be considered for the proper design of detection and mitigation systems dealing with the investigated species to limit the occurrence of conditions potentially leading to fire spreading. From a phenomenological point of view, the vaporization was identified as the rate-determining step of the liquid-gas reactive system once a flaming regime was observed. Hence, the collected data can be also adopted for the validation and refinement of advanced numerical calculations and models of liquid-vapour reactive systems. Based on the highlighted information, these findings enhance the understanding of the fire behaviour of liquid solvents suitable for energy storage systems and contribute to the development of improved fire safety measures and mitigation strategies as well as to the optimization of technological solutions involving the energy sector during the design phase. In addition, the collected database can be considered for the development of dedicated models and the realization of advanced numerical evaluations of the safety aspects involving case-specific scenarios and conditions employing liquid flammable species.

CRediT authorship contribution statement

Ernesto Salzano: Funding acquisition, Supervision, Writing – review & editing. **Gianmaria Pio:** Conceptualization, Methodology, Supervision, Validation, Writing – review & editing. **Benedetta De Liso:** Data curation, Formal analysis, Investigation, Writing – original draft.

Declaration of Competing Interest

The authors declare that they have no known competing financial interests or personal relationships that could have appeared to influence the work reported in this paper.

Acknowledgement

Authors gratefully acknowledge the Italian Ministry of University and Research (MIUR) for the financial support through the National Recovery and Resilience Plan (PNRR), Mission 4, Component 2, Investment 1.3, NextGenerationEU, Extended Partnership PE2: NEST – Network 4 Energy Sustainable Transition", Spoke 6: Energy Storage - T6.4.4 Safety, LCA and sustainability studies of energy storage systems and processes, Grant number PE00000021, CUPJ33C22002890007.

References

An, W., Jiang, L., Sun, J., Liew, K.M., 2015. Correlation analysis of sample thickness, heat flux, and cone calorimetry test data of polystyrene foam. J. Therm. Anal. Calorim. 119, 229–238. https://doi.org/10.1007/s10973-014-4165-9.

ASTM, A.S. for T. and M, 2023. ASTM E1354-23 - Standard Test Method for Heat and Visible Smoke Release Rates for Materials and Products Using an Oxygen Consumption Calorimeter.

Babrauskas, V., 1984. Development of the cone calorimeter?A bench-scale heat release rate apparatus based on oxygen consumption. Fire Mater. 8, 81–95. https://doi.org/10.1002/fam.810080206.

Babrauskas, V., 1989. Smoke and gas evolution rate measurements on fire-retarded plastics with the cone calorimeter. Fire Saf. J. 14, 135–142. https://doi.org/10.1016/0379-7112(89)90067-2.

Ben Talouba, I., Balland, L., Mouhab, N., Bensahla, N., 2018. Kinetic and safety parameters of decomposition of neat Tert-Butyl (2-Ethylhexyl) monoperoxy Carbonate and in organic solvents. Thermochim. Acta 659, 105–112. https://doi.org/10.1016/j.tca.2017.09.022.

Beyler, C., 2003. Flammability limits of premixed and diffusion flames. SFPE Handb. Fire Prot. Eng. https://doi.org/10.1007/978-1-4939-2565-0.

Bray, R.J., Tretsiakova-McNally, S., Zhang, J., 2023. The controlled atmosphere cone calorimeter: a literature review. Fire Technol. https://doi.org/10.1007/s10694-023-01423-6.

British Standards Institution, 2019. ISO 5660-1: 2019. Reaction-to-fire tests. Heat release, smoke production and mass loss rate Heat release rate (cone calorimeter method) and smoke production rate (dynamic measurement).

Brohez, S., Delvosalle, C., Marlair, G., Tewarson, A., 2000. The measurement of heat release from oxygen consumption in sooty fires. J. Fire Sci. 18, 327–353. https://doi.org/10.1177/073490410001800501.

Broustail, G., Seers, P., Halter, F., Moréac, G., Mounaim-Rousselle, C., 2011. Experimental determination of laminar burning velocity for butanol and ethanol iso-octane blends. Fuel 90, 1–6. https://doi.org/10.1016/j.fuel.2010.09.021.

Bu, Y., Wu, Y., Li, X., Pei, Y., 2023. Operational risk analysis of a containerized lithium-ion battery energy storage system based on STPA and fuzzy evaluation. Process Saf. Environ. Prot. 176, 627–640. https://doi.org/10.1016/j.psep.2023.06.023.

Cameo, 2023. CAMEO Chemicals [WWW Document]. URL ⟨https://cameochemicals.noaa.gov/⟩.

Cao, J., Ju, X., Peng, Y., Zhou, X., Hu, Y., Li, L., Wang, D., Cao, B., Yang, L., Peng, F., 2020. Experimental study on fire hazard of LiCoO2-based lithium-ion batteries with gel electrolyte using a cone calorimeter. J. Energy Storage 32, 101884. https://doi.org/10.1016/j.est.2020.101884.

Chai, S., Zhang, Y., Wang, Y., He, Q., Zhou, S., Pan, A., 2022. Biodegradable composite polymer as advanced gel electrolyte for quasi-solid-state lithium-metal battery. eScience 2, 494–508. https://doi.org/10.1016/j.esci.2022.04.007.

Chakrabarty, A., Mannan, S., Cagin, T., 2016. Finite Element Analysis in Process Safety Applications. in: Multiscale Modeling for Process Safety Applications. Elsevier, pp. 275–288. https://doi.org/10.1016/B978-0-12-396975-0.00005-X.

Cheng, H., Zhang, S., Zhang, B., Lu, Y., 2023. n -hexane diluted electrolyte with ultralow density enables Li–S pouch battery toward >400 Wh kg −1. Small 19, 2206375. ⟨https://doi.org/10.1002/smll.202206375⟩.

Coronel, S., Mével, R., Vervish, P., Boettcher, P.A., Thomas, V., Chaumeix, N., Darabiha, N., Shepherd, J.E., 2013. Laminar burning speed of n-hexane-air mixtures. 8th US Natl. Combust. Meet. 2013 (3), 2568–2583.

Crowl, D.A., Britton, L.G., Frank, W.L., Grossel, S., Hendershot, D., High, W.G., Johnson, R.W., Kletz, T.A., Leung, J.C., Moore, D.A., Ormsby, R., Prugh, Ri.W., Owens, J.E., Siwek, R., Spicer III, T.O., Summers, A., Willey, R., Woodward, J.L., 2008. Perry's chemical engineers'. Handb. Sect. 23 Process Saf. https://doi.org/10.1036/0071542051.

DiDomizio, M.J., Ibrahimli, V., Weckman, E.J., 2021. Testing of liquids with the cone calorimeter. Fire Saf. J. 126, 103449 https://doi.org/10.1016/j.firesaf.2021.103449.

Ferek, R.J., Reid, J.S., Hobbs, P.V., Blake, D.R., Liousse, C., 1998. Emission factors of hydrocarbons, halocarbons, trace gases and particles from biomass burning in Brazil. J. Geophys. Res. Atmos. 103, 32107–32118. https://doi.org/10.1029/98JD00692.

Fernandes Oliveira, R.L., Doubek, G., Vianna, S.S.V., 2019. On the behaviour of the temperature field around pool fires in controlled experiment and numerical modelling. Process Saf. Environ. Prot. 123, 358–369. https://doi.org/10.1016/j.psep.2018.12.031.

Gavelli, F., Bullister, E., Kytomaa, H., 2008. Application of CFD (Fluent) to LNG spills into geometrically complex environments. J. Hazard. Mater. 159, 158–168. https://doi.org/10.1016/j.jhazmat.2008.02.037.

Gu, X.J., Haq, M.Z., Lawes, M., Woolley, R., 2000. Laminar burning velocity and Markstein lengths of methane-air mixtures. Combust. Flame. https://doi.org/10.1016/S0010-2180(99)00142-X.

Hagen, B.C., Meyer, A.K., 2021. From smoldering to flaming fire: different modes of transition. Fire Saf. J. 121, 103292 https://doi.org/10.1016/j.firesaf.2021.103292.

Incropera, F.P., Dewitt, D.P., Bergamm, T.L., Lavine, A.S., 2007. Fundamentals of heat and mass transfer, sixth ed. John Wiley and Sons, Hoboken, USA.

Janošovský, J., Rosa, I., Vincent, G., Šulgan, B., Variny, M., Labovská, Z., Labovský, J., Jelemenský, Ľ., 2022. Methodology for selection of inherently safer process design alternatives based on safety indices. Process Saf. Environ. Prot. 160, 513–526. https://doi.org/10.1016/j.psep.2022.02.043.

Janssens, M., 1991. Piloted ignition of wood: a review. Fire Mater. 15, 151–167. https://doi.org/10.1002/fam.810150402.

Kumar, R., Priyadarshani Padhi, U., Kumar, S., 2023. Laminar burning velocity measurements of ethyl acetate at higher mixture temperatures. Fuel 338, 127278. https://doi.org/10.1016/j.fuel.2022.127278.

Lin, X., Khosravinia, K., Hu, X., Li, J., Lu, W., 2021. Lithium plating mechanism, detection, and mitigation in lithium-ion batteries. Prog. Energy Combust. Sci. 87, 100953 https://doi.org/10.1016/j.pecs.2021.100953.

Linstrom, P.J., Mallard, W.G., 2014. NIST Chemistry webBook. In: NIST Standard Reference Database Number, 69. Natl. Inst. Stand. Technol.

Logan, E.R., Tonita, E.M., Gering, K.L., Li, J., Ma, X., Beaulieu, L.Y., Dahn, J.R., 2018. A study of the physical properties of Li-Ion battery electrolytes containing esters. J. Electrochem. Soc. 165, A21–A30. https://doi.org/10.1149/2.0271802jes.

Marsh, N.D., Gann, R.G., 2013. Smoke component yields from Bench-Scale Fire Tests (Gaithersburg, MD). ISO 5660-1 / ASTM E 1354 Enclos. Var. Oxyg. Conc. 3. https://doi.org/10.6028/NIST.TN.1762.

Marshall, S.P., Taylor, S., Stone, C.R., Davies, T.J., Cracknell, R.F., 2011. Laminar burning velocity measurements of liquid fuels at elevated pressures and temperatures with combustion residuals. Combust. Flame 158, 1920–1932. https://doi.org/10.1016/j.combustflame.2011.02.016.

McGrath, D., Fan, L., Gkantonas, S., Hochgreb, S., 2023. The effect of fuel droplets on the burning velocity of strained laminar acetone/air flames. Proc. Combust. Inst. 39, 2503–2511. https://doi.org/10.1016/j.proci.2022.07.133.

Mun, S.Y., Cho, J.H., Hwang, C.H., 2021. Effects of external heat flux and exhaust flow rate on co and soot yields of acrylic in a cone calorimeter. Appl. Sci. 11 https://doi.org/10.3390/app11135942.

Perry, R.H., Poling, B.E., Thomson, G.H., Friend, D.G., Rowley, R.L., Wilding, W.V., 2007. Perry's Chemical Engineers' Handbook - Section 2: Physical and Chemical Data, 8th ed, Perry's Chemical Engineers' Handbook. United State of America. https://doi.org/10.1036/0071511253.

Pio, G., Salzano, E., 2018. Evaluation of safety parameters of light alkenes by means of detailed kinetic models. Process Saf. Environ. Prot. 119, 131–137. https://doi.org/10.1016/j.psep.2018.07.024.

Rantuch, P., Martinka, J., Ház, A., 2021. The evaluation of torrefied wood using a cone calorimeter. Polym. (Basel) 13, 1748. https://doi.org/10.3390/polym13111748.

Salzano, E., Pio, G., Ricca, A., Palma, V., 2018. The effect of a hydrogen addition to the premixed flame structure of light alkanes. Fuel 234, 1064–1070. https://doi.org/10.1016/j.fuel.2018.07.110.

Sung, K., Chen, J., Bundy, M., Hamins, A., 2021. The characteristics of a 1 m methanol pool fire. Fire Saf. J. 120, 103121 https://doi.org/10.1016/j.firesaf.2020.103121.

Tan, P., Kong, W., Shao, Z., Liu, M., Ni, M., 2017. Advances in modeling and simulation of Li–air batteries. Prog. Energy Combust. Sci. 62, 155–189. https://doi.org/10.1016/j.pecs.2017.06.001.

Tang, J., Wu, X., Ren, J., Min, H., Liu, X., Kong, Y., Che, P., Zhai, W., Yang, H., Shen, X., 2023. Suppressing thermal runaway propagation of nickel-rich Lithium-ion battery modules using silica aerogel sheets. Process Saf. Environ. Prot. 179, 199–207. https://doi.org/10.1016/j.psep.2023.08.100.

Vesovic, V., 2007. The influence of ice formation on vaporization of LNG on water surfaces. J. Hazard. Mater. 140, 518–526. https://doi.org/10.1016/j.jhazmat.2006.10.039.

Wang, S., Wang, Z., He, Y., Han, X., Sun, Z., Zhu, Y., Costa, M., 2020. Laminar burning velocities of CH4/O2/N2 and oxygen-enriched CH4/O2/CO2 flames at elevated pressures measured using the heat flux method. Fuel 259, 116152. https://doi.org/10.1016/j.fuel.2019.116152.

Ward, D.E., Hardy, C.C., 1991. Smoke emissions from wildland fires. Environ. Int. 17, 117–134. https://doi.org/10.1016/0160-4120(91)90095-8.

Winter, M., Brodd, R.J., 2004. What are batteries, fuel cells, and supercapacitors? Chem. Rev. 104, 4245–4270. https://doi.org/10.1021/cr020730k.

Yamada, Y., Furukawa, K., Sodeyama, K., Kikuchi, K., Yaegashi, M., Tateyama, Y., Yamada, A., 2014. Unusual stability of acetonitrile-based superconcentrated electrolytes for fast-charging lithium-ion batteries. J. Am. Chem. Soc. 136, 5039–5046. https://doi.org/10.1021/ja412807w.

Yin, L., Xu, W., Hu, Y., Jiang, Y., 2023. Experimental and theoretical investigation of ethyl methyl carbonate/air flames: Laminar burning velocity and cellular instability at elevated pressures. Fuel 346, 128206. https://doi.org/10.1016/j.fuel.2023.128206.

Zhai, J., Sun, X., Huang, S., Xie, H., Chen, X., 2023. Economic, thermodynamic, environmental, and inherent safety investigation of heat pump-assisted extractive dividing wall column for separating binary azeotrope. Process Saf. Environ. Prot. 173, 202–214. https://doi.org/10.1016/j.psep.2023.03.027.

Zhang, W., Sun, H., Hu, P., Huang, W., Zhang, Q., 2021. Double-effect of highly concentrated acetonitrile-based electrolyte in organic lithium-ion battery. EcoMat 3. https://doi.org/10.1002/eom2.12128.